

Magnetic and corrosion resistance properties of NdFeBCo magnets fabricated using underwater shock compaction

Youngkook Kim^{*}, Shigeru Itoh^{**} and Chai-Bong Lee^{***†}

^{*}Shock Wave and Condensed Matter Research Center, Kumamoto University
2-39-1 Kurokami, Kumamoto City, Kumamoto, 860-8555, Japan

^{**}Okinawa National College of Technolgy, 905 Henoko, Nago, Okinawa 905 -2192, Japan

^{***}Dept. of Electronics Engineering, Dongseo University
San 69-1, Jurye-2dong, Sasang-gu, Busan 617-716, South Korea
Phone +82-51-320-1755

[†]Corresponding address : lcb@gdsu.dongseo.ac.kr

Received : January 31, 2012 Accepted : March 2, 2012

Abstract

NdFeBCo magnets were fabricated using underwater shock compaction, and their magnetic, mechanical and corrosion resistance properties were investigated. Cracks and voids were seen to form in the shock-consolidated magnets and increased with increasing cobalt (Co) additions. Magnetization also decreased with increasing Co additions; however, coercivity increased. Regarding corrosion resistance, a shock-consolidated NdFeB magnet without Co addition showed faster oxidation velocity than compacts with Co additions. Regarding hardness value, NdFeBCo with Co addition of 5% addition showed a sharp increase; however, the value decreased when Co addition exceeded 10%.

Keywords : underwater shock compaction, NdFeB magnet, corrosion resistance

1. Introduction

Many types of rare-earth permanent magnets which possess high magnetic properties are based on SmCo₅, Nd₂Fe₁₄B or Sm₂Fe₁₇N_x alloys. These magnetic materials are fabricated by techniques such as powder metallurgical sintering process¹⁾⁻³⁾, melt-spinning route⁴⁾⁻⁷⁾, mechanically alloying process⁸⁾⁻¹¹⁾ and hot working technique¹²⁾⁻¹³⁾ to obtain high remanence, coercivity and energy product.

Generally, the multi-component composition of magnets leads to the formation of nonmagnetic and soft magnetic phases, and the composition can change the intrinsic properties such as Curie temperature, magneto-crystalline anisotropy and even corrosion resistance¹⁴⁾. The usage of Nd-Fe-B sintered magnets has dramatically increased over the years since their development¹⁵⁾ because of their high magnetic properties. Permanent magnets based on Nd-Fe-B have contributed to new applications such as electric appliances, automobiles and industrial motors¹⁶⁾. Nd-Fe-B

based permanent magnets exhibit complex multi-phase microstructures such as a hard magnetic Nd₂Fe₁₄B phase, boride NdFe₄B₄ phase, and low melting Nd-rich phase located in the intergranular region. Also, because Nd-Fe-B based permanent magnets are very sensitive to oxidization, considerable research has been directed at improving corrosion resistance¹⁷⁾⁻¹⁹⁾. Recently, polymer bonded magnets based on Nd-Fe-B alloys have seized sizable market share in the rapidly growing magnet industry. However, Plusa *et al.*²⁰⁾ reported that Nd-Fe-B bonded magnets exhibit lower remanence (M_R) and maximum energy product $(BH)_{max}$ because of their lower volume fraction. These bonded magnets are manufactured by means of compression or injection molding process.

The underwater shock compaction technique²¹⁾⁻²⁵⁾ is a promising method for magnetic powder consolidation. This technique avoids prolonged heat treatment and fabricates a denser bulk without the use of a binder due to

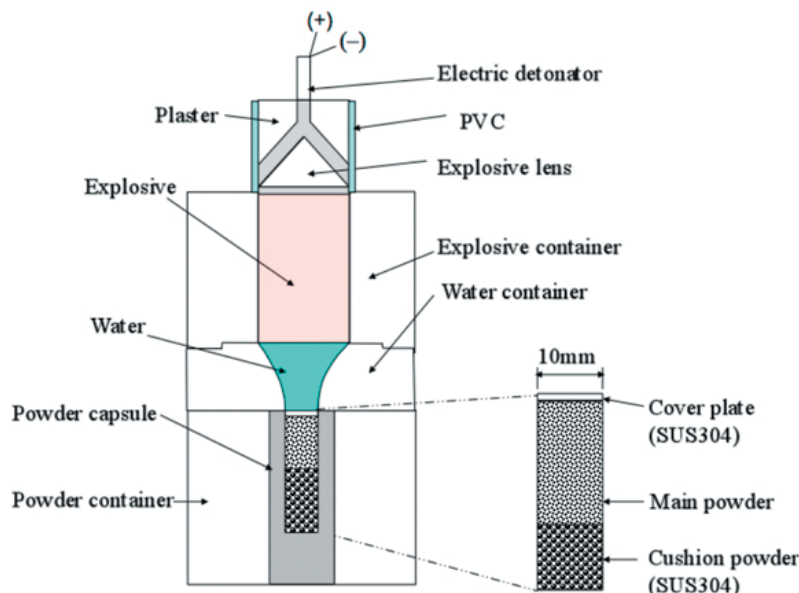


Figure 1 Schematic illustration of powder consolidation device

its very fast consolidation process and high shock pressure. In this study, we have employed the underwater shock compaction technique to fabricate Nd-Fe-B bulk magnets with cobalt (Co) additions with the aim of investigating magnetic, mechanical and corrosion resistance properties of shock-consolidated Nd-Fe-B-Co magnets.

2. Experimental procedure

The powder consolidation device, shown in Figure 1, consists of an explosive container, water container, powder container and powder capsule. A high performance explosive, water and powder were charged and filled to each container. The main powders used in this study were $\text{Nd}_2\text{Fe}_{14}\text{B}$ powder ($\leq 350\ \mu\text{m}$ particle size) and Co powder ($\leq 45\ \mu\text{m}$ particle size). Co powder ratios of 5%, 10% and 15% were respectively added to the $\text{Nd}_2\text{Fe}_{14}\text{B}$ powder. The mixed Nd-Fe-B-Co powders were press-inserted to the powder capsule using a uniaxial press machine (at $20\ \text{kgf}/\text{cm}^2$) under argon atmosphere. To eliminate the influence of a reflected force, a cushion powder (SUS304, $\leq 45\ \mu\text{m}$ particle size) was used.

To investigate the corrosion resistance of the shock-consolidated Nd-Fe-B-Co magnets, thermogravimetric analysis (TGA) tests were performed on samples weighing approximately 0.3 g using a TGA-60 measurement device under atmosphere test conditions. The samples were heated from ambient temperature to the set point of 700°C at a heating rate of $10^\circ\text{C}/\text{min}$. Weight changes were recorded automatically.

Magnetic property measurements of shock-consolidated Nd-Fe-B-Co magnets with a weight of 1.7 mg were performed using a commercial super conducting quantum interference device (SQUID) magnetometer.

3. Results and discussion

Figure 2 shows photographs of shock-consolidated Nd-Fe-B and Nd-Fe-B-Co magnets. The compacts were mechanically processed using machine tools, and their

relative densities for the theoretical density were about 96 ~97%. Figure 3 shows optical microscope images of the NdFeBCo compacts versus those with Co additions. It was confirmed that the mixed Nd-Fe-B-Co powders are completely melted, and cracks, voids and pores are formed. Cracking and voiding problems often occur in shock compaction since high velocity impact and tensile waves easily induce cracks in the compacts²⁶. The compacts showed increased cracking and voiding with increasing Co additions, possibly caused by the difference in hardness and thermal expansion properties between the Co element and Nd-rich phase distributed on the grain boundary area. The X-ray diffraction (XRD) analysis shown in Figure 4 reveals that the Nd-rich phase very quickly oxidizes and changes to Nd_2O_3 phases in all compacts. Figure 5 shows the magnetization curves versus the magnetic field at 1 T (Tesla) measured by SQUID magnetometer for the shock-consolidated Nd-Fe-B and Nd-Fe-B-Co magnets, revealing that the magnetization saturation point decreased with increasing Co additions. This is caused by cracks, voids and some lattice defects which were generated by high velocity impact. Therefore, shock compaction can be expected to lead to a decrease in magnetization, and Co powder can become an impurity suppressing magnetization if there is no perfect chemical combination between the Co powder and Nd-Fe-B powder. Coercivity showed an unusual increase with increasing Co additions, as shown in Figure 6, increasing up to the ratio of Co 10% addition and then decreased at the ratio of Co 15% addition. This is related to the generation of a new magnetic phase in the nonmagnetic Nd-rich phase where excessive Co additions are made and is consistent with previously reports²⁷. In addition, coercivity is affected by domain wall trap structures²⁸; micro-cracks, voids, pores and impurities can lead to an increase in domain wall trap energy, which can influence the increase of coercivity. Specifically, shock compaction effects an increase in coercivity since voids and pores are easily generated. Figure 7 shows the results

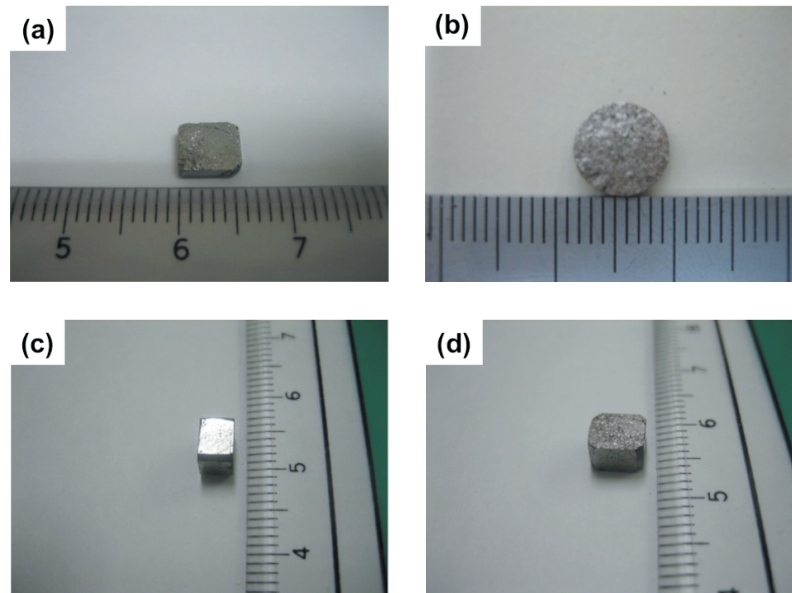


Figure 2 Photographs of (a) shock-consolidated Nd-Fe-B; (b) Nd-Fe-B- (Co 5%); (c) Nd-Fe-B- (Co 10%); (d) Nd-Fe-B- (Co 15%) magnets.

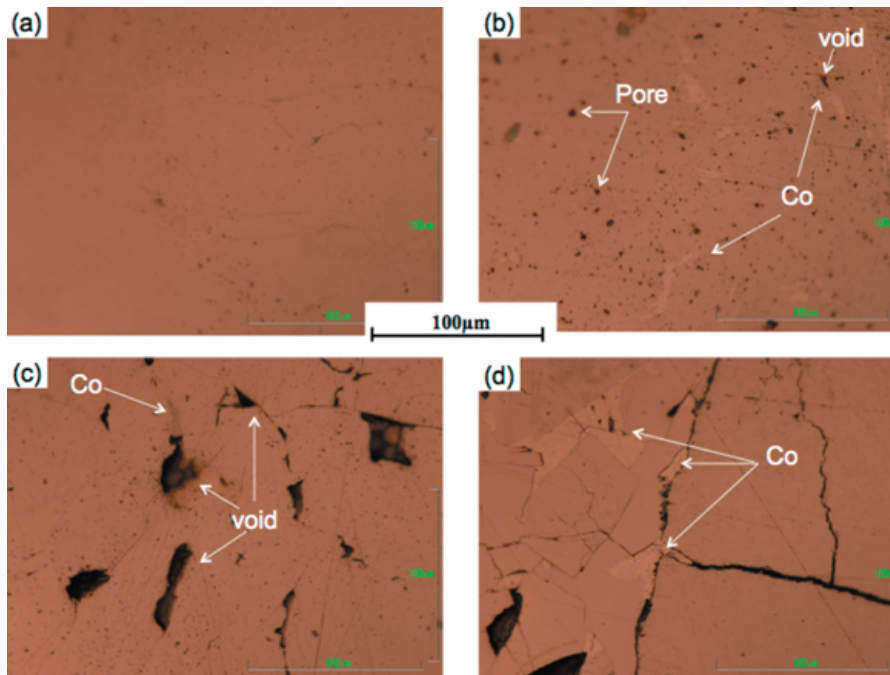


Figure 3 Optical microscope images of (a) shock-consolidated Nd-Fe-B; (b) Nd-Fe-B- (Co 5%); (c) Nd-Fe-B- (Co 10%); (d) Nd-Fe-B- (Co 15%) magnets.

of thermogravimetric analysis (TGA) tests for the shock-consolidated Nd-Fe-B and Nd-Fe-B-Co (Co 5%, 10% and 15% additions). The weight change versus the temperature change was investigated. The Nd-Fe-B compact exhibited a rapid weight change, and its oxidation velocity was faster than the Nd-Fe-B-Co compacts, which have a gentle weight change with increasing Co additions. This is evidence that the corrosion resistance of Nd-Fe-B has improved by the Co additions. For the hardness values of Nd-Fe-B-Co compacts as shown in Figure 8, all samples exhibited higher hardness values than that of powder metallurgical sintered Nd-Fe-B magnets (H_v 527~568)²⁹. In the case of Co 5% additions, the hardness sharply increased due to strengthened intergranular phases²⁹. However, hardness of the

NdFeBCo with Co 10% and 15% addition decreased.

4. Conclusions

Shock-consolidated Nd-Fe-B-Co magnets were fabricated using the underwater shock compaction technique. Shock-consolidated samples showed that crack formation increased with increasing Co additions due to differences in hardness and thermal expansion coefficients between the Co element and Nd-rich phases, which is distributed on the grain boundary area and can lead to difficulties in powder compaction. Regarding magnetic properties, the saturated magnetization point and magnetic permeability also decreased with increasing Co additions. However, coercivity increased up to the ratio of Co 10% addition before decreasing at the ratio of Co 15%.

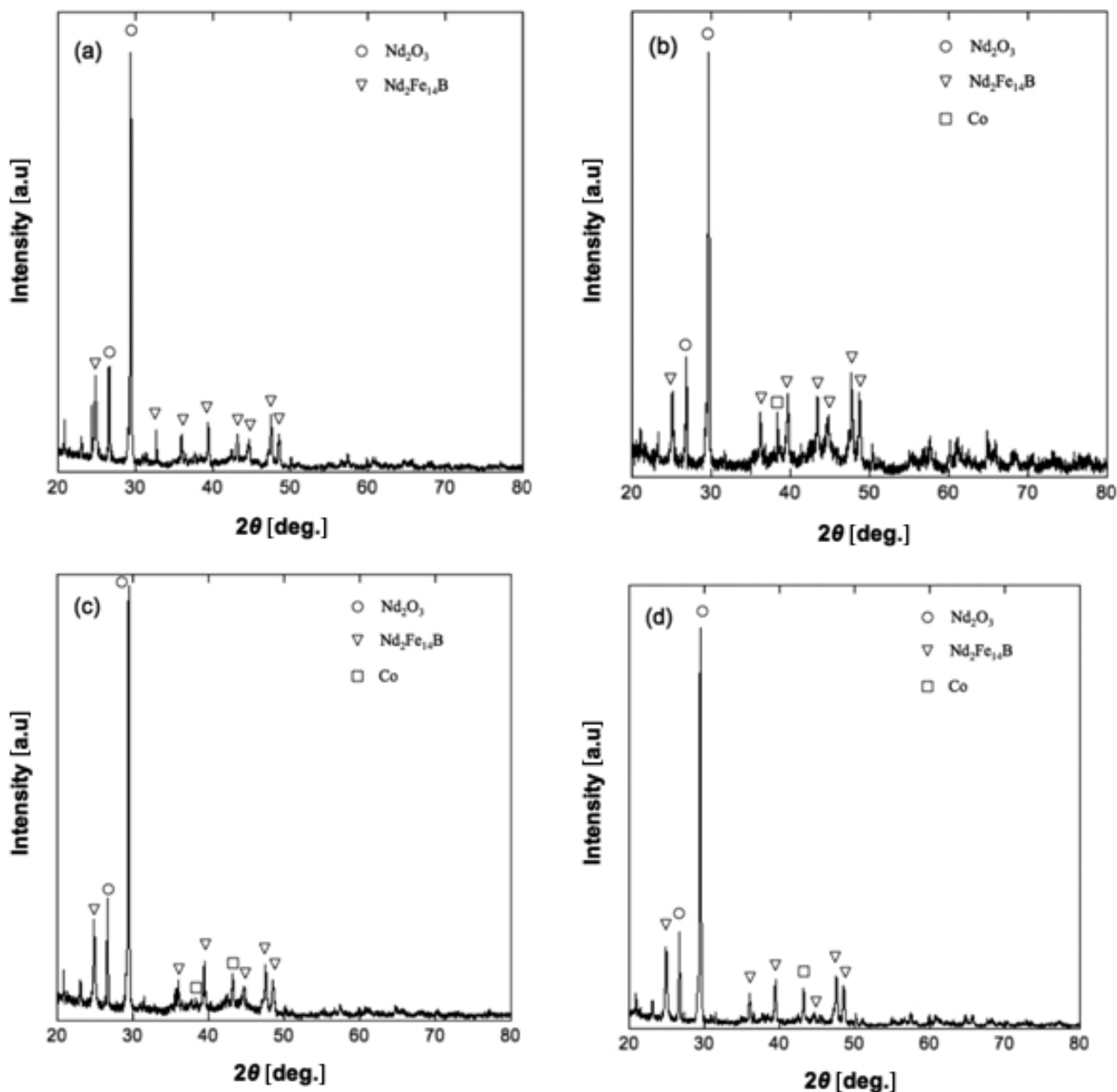


Figure 4 X-ray peak patterns of (a) shock-consolidated Nd-Fe-B; (b) Nd-Fe-B- (Co 5%); (c) Nd-Fe-B- (Co 10%); (d) Nd-Fe-B- (Co 15%) magnets.

This increase in coercivity is affected by the domain wall trap energy, which is generated by impurities, voids and cracks. In the case of Co addition of 15%, coercivity decreased due to the generation of a new magnetic phase in the nonmagnetic Nd-rich phase, where excessive Co additions are made.

Regarding corrosion resistance, the shock-consolidated Nd-Fe-B magnet without Co addition showed an increase in weight compared to that of the shock-consolidated Nd-Fe-B-Co magnets with the Co additions because nonmagnetic Nd-rich phase is very sensitive to oxidation. The corrosion resistance of shock-consolidated Nd-Fe-B-Co was shown to improve with increasing the Co additions. Hardness sharply increased in the case of Co 5% addition because the intergranular phase was strengthened.

References

- 1) J. Tian, X. Qu, S. Zhang, D. Cui, and F. Akhtar, *Mater. Lett.* 61 5271–5274 (2007).
- 2) Y. Ding, R. J. Chen, Z. Liu, D. Lee, and A. R. Yan, *J. Appl. Phys.* 107, 09A726 (2010).
- 3) L. Krone, E. Schüller, M. Bram, O. Hamed, H.-P. Buchkremer, and D. Stöver, *Mater. Sci. Eng. A* 378, 185–190 (2004).
- 4) J. J. Croat, J. F. Herbst, R. W. Lee, and F. E. Pinkerton, *J. Appl. Phys.*, 55, 2078–2083 (1984).
- 5) J. J. Croat, *J. Appl. Phys.* 53, 3161–3169 (1982)
- 6) T. Saito, W. Q. Wang, and Y. Kamagata, *J. Alloys and Compounds* 402, 242–245 (2005).
- 7) K. Suresh, R. Gopalan, A.K. Singh, G. Bhikshamaiah, V. Chandrasekaran, and K. Honoc, *J. Alloys and Compounds* 436, 358–363 (2007).
- 8) C. Kuhrt, and Schultz, *J. Appl. Phys.* 73, 6588–6590 (1993).
- 9) T. Harada, T. Kuji, *J. Alloys and Compounds* 232, 238–246 (1996).
- 10) Y. V. Baldokhin, V. V. Tcherdyntsev, S. D. Kaloshkin, G. A. Kochetov, and Y. A. Postov, *J. Magn. Magn. Mater.* 203, 313

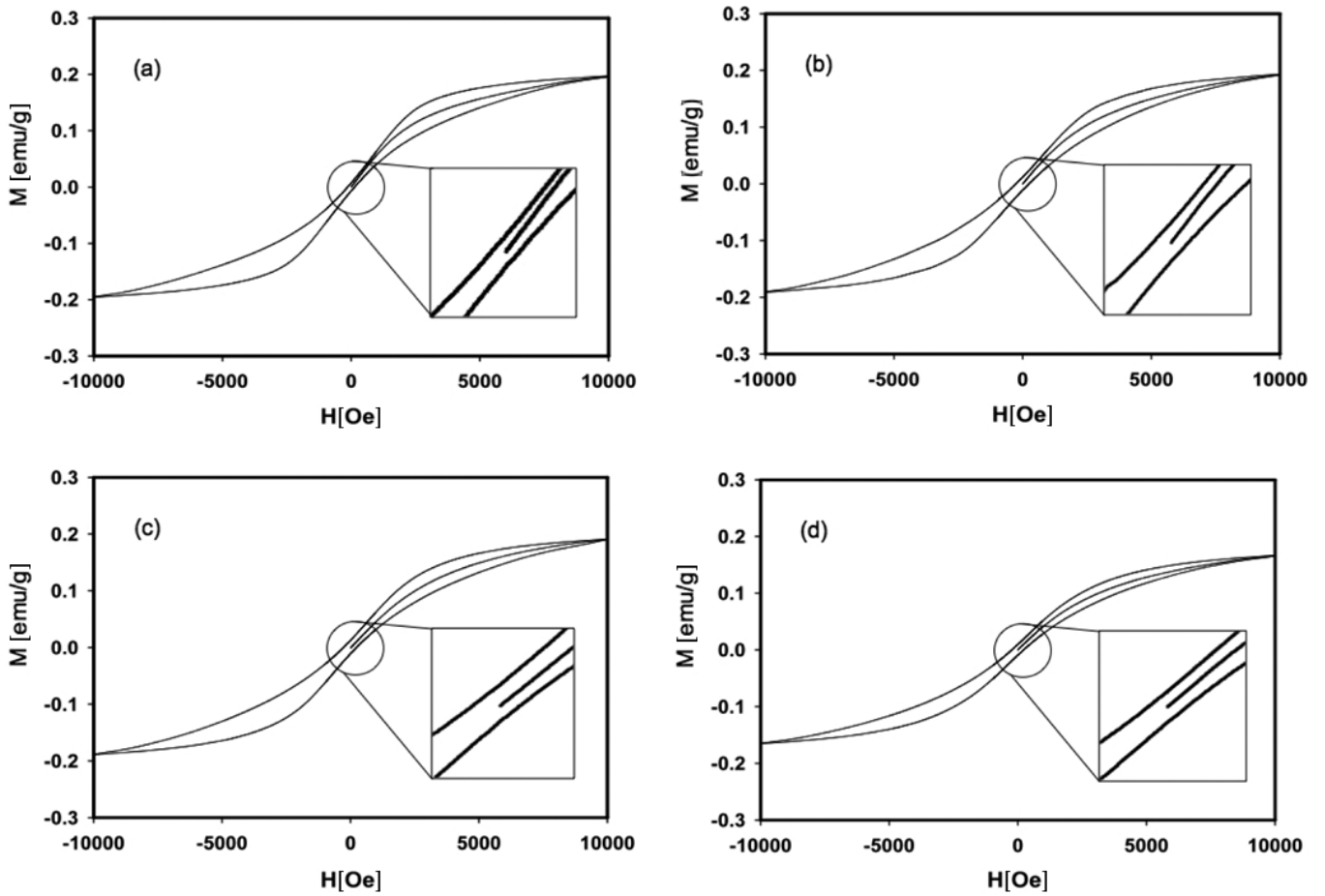


Figure 5 Magnetization curves vs. magnetic field for the (a) shock-consolidated Nd-Fe-B; (b) Nd-Fe-B- (Co 5%); (c) Nd-Fe-B- (Co 10%); (d) Nd-Fe-B- (Co 15%) magnets.

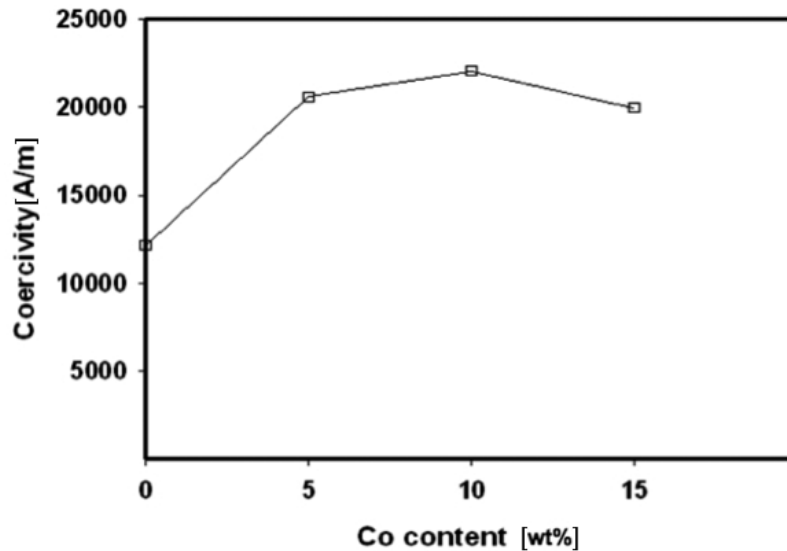


Figure 6 Coercivity of shock-consolidated Nd-Fe-B and Nd-Fe-B-Co magnets with Co additions.

–315 (1999).

11) G. González, D. Ibarra, J. Ochoa, R. Villalba, and A. Sagarzazu, *J. Alloys and Compounds* 434, 437–441 (2007).

12) R. W. Lee, E. G. Brewer and N. A. Schaffel, *IEEE Trans. Magn. Mag.* 21, 1958–1963 (1985).

13) J. P. Nozières, R. Perrier de la Bâthie, and D. W. Taylor, *J. Magn. Magn. Mater.*, 80, 88–92 (1989).

14) S. Sunada, K. Majima, Y. Akasofu, and Y. Kaneko, *J. Alloys and Compounds* 408, 1373–1376 (2006).

15) M. Sagawa, S. Fujimura, N. Togawa, H. Yamamoto, Y. Matsuura, *J. Appl. Phys.* 55, 2083–2087 (1984).

16) Y. Matsuura, *J. Magn. Magn. Mater.*, 303, 344–347 (2006).

17) W. Fernengel, W. Rodewald, R. Blank, P. Schrey, M. Katter, and B. Wall, *J. Magn. Magn. Mater.*, 196, 288–290 (1997).

18) W. Kaszuwara, M. Leonowicz, and S. Wojciechowski, *Mater. Lett.* 24, 341–345 (1995).

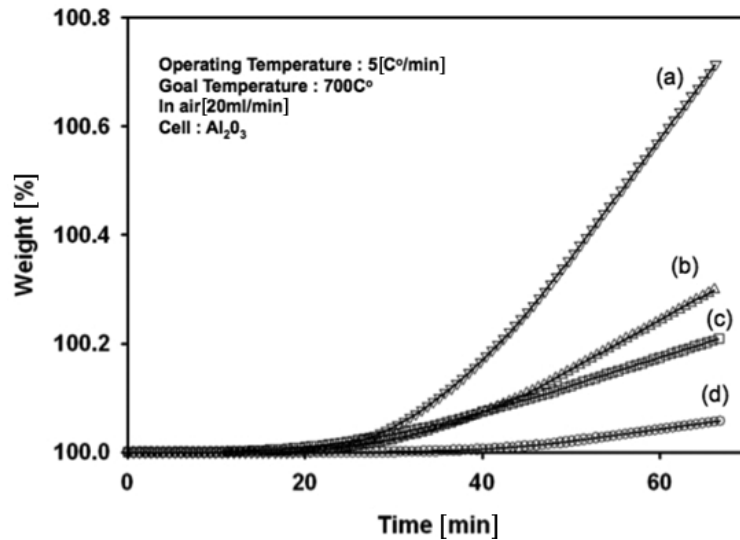


Figure 7 Weight change curves with increasing temperature for the (a) shock-consolidated Nd-Fe-B; (b) Nd-Fe-B (Co 5%); (c) Nd-Fe-B (Co 10%); (d) Nd-Fe-B (Co 15%) magnets.

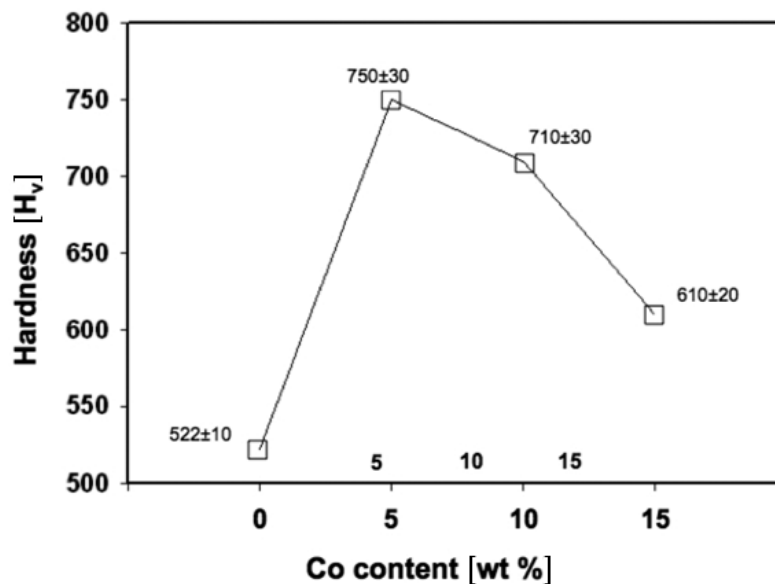


Figure 8 Hardness values of shock-consolidated Nd-Fe-B and Nd-Fe-B (Co 5%, 10%, 15%) magnets.

- 19) A. M. Gabay, Y. Zhang, and G. C. Hadjipanayis, *J. Magn. Magn. Mater.*, 238, 226–232 (2002).
- 20) D. Plusa, M. Dospial, B. Slusarek, and U. Kotlarczyk, *J. Magn. Magn. Mater.*, 306, 302–308 (2006).
- 21) Y. Kim, T. Ueda, K. Hokamoto, and S. Itoh, *Ceram. Int.* 35, 3247–3252 (2009).
- 22) Y. Kim, T. Ikegami, and S. Itoh, *Powder Technol.*, 208, 575–581 (2011).
- 23) Y. Kim, F. Mitsugi, T. Ikegami, K. Hokamoto, and S. Itoh, *J. Eur. Ceram. Soc.*, 31, 1033–1039 (2011).
- 24) Y. Kim, H. Wada, Y. Lee, and S. Itoh, *Mater. Sci. Eng. B*, 167, 114–118 (2010).
- 25) A. Chiba, S. Kimura, K. Raghukandan, and Y. Morizono, *Mater. Sci. Eng. A* 350, 179–183 (2003).
- 26) M. A. Meyers, D. J. Benson, and E. A. Olevsky, *Acta Mater.* 47, 2089–2108 (1999).
- 27) S. Arai, T. Shibata and M. Nagakura, *Meiji University, Memoirs of the Institute of Sciences and Technology*, 24, 1–19 (1985).
- 28) M. C. Chi, E. M. Gyorgy, and R. Alben, *J. Appl. Phys.* 49, 2016–2018 (1978).
- 29) J. Jiang, Z. Zeng, J. Yu, J. Wu, and M. Tokunaga, *Intermetallics* 9, 269–272 (2001).